Geomorphology 457 (2024) 109231

Contents lists available at ScienceDirect

Geomorphology

journal homepage: www.journals.elsevier.com/geomorphology

Combining terrestrial lidar with single line transects to investigate geomorphic change: A case study on the Upper Verde River, Arizona

Lauren L. Tango [a,b], Temuulen Ts. Sankey [b,*], Jackson Leonard [c], Joel B. Sankey [a], Alan Kasprak [d]

[a] U.S. Geological Survey, Southwest Biological Science Center, Grand Canyon Monitoring and Research Center, 2255 N. Gemini Dr. Flagstaff, AZ, 86001, USA
[b] School of Informatics, Computing and Cyber Systems, Northern Arizona University, 1295 S Knoles Dr. Flagstaff, AZ, 86011. USA
[c] U.S. Forest Service, Rocky Mountain Research Station, 2500 S Pine Knoll Dr. Flagstaff, AZ, 86001. USA
[d] Fort Lewis College, Department of Geosciences, 1000 Rim Dr. Durango, CO, 81301. USA

ARTICLE INFO

Keywords:
Terrestrial Lidar
Remote Sensing
Fluvial Geomorphology
Change Detection
Statistical Analysis

ABSTRACT

The Upper Verde River in northern Arizona, USA is a vital resource for the wildlife and humans that rely on its waters. We characterize the riparian corridor topography using terrestrial laser scanner (TLS) data from 2021 to 2022. We also quantify geomorphic changes associated with human and climate-driven alterations in river flow and vegetation changes by combining the contemporary lidar surveys with legacy measurements from single line geomorphology transects measured by the United States Forest Service (USFS) in 2009. Seventeen plots along the Upper Verde River were surveyed with the TLS and the data were coregistered within individual plots with a Root Mean Square Error of <0.03 m among scan positions. Digital Elevation Models (DEM) were derived for each plot from the TLS data at 10 cm resolution and compared to the 2009 USFS cross-section data to quantify elevation changes. In areas with statistically significant change, we detected maximum changes in elevation due to erosion and deposition of -0.37 m and $+0.97$ m, respectively. Topographic changes over the 13-year period were predominately aggradation and associated with sediment deposition, which we hypothesize might have resulted from altered river flow and vegetation encroachment. This study also demonstrates a quantitative and statistical methodology to fuse traditional single line cross-section data with contemporary lidar data to quantify geomorphic change. The novel approach demonstrated here is broadly applicable to natural resource managers for integrating and contextualizing legacy topographic data for understanding past, present, and future landscape and habitat changes.

1. Introduction

Rivers are vital to ecosystem and human health, water security, and ecosystem resilience (East and Sankey, 2020; Fries et al., 2020; Stromberg and Stevens, 2008). Desert rivers, often referred to as “ribbons of life” (Mott Lacroix et al., 2017; Zaimes et al., 2007), provide crucial resources for the survival of native riparian plants and animals, including livestock and wildlife, and their habitats. Climate change and the current megadrought in the American Southwest have already had substantial and irreversible impacts on terrestrial freshwater ecosystems and on the health of rivers in the region (Pörtner et al., 2022). River flows in the region are projected to decrease (Overpeck and Udall, 2020), and runoff regimes might drastically change due to climate variability and human consumption of water (Ellis et al., 2008; Udall and Overpeck, 2017).

The Upper Verde River (UVR), located in northern Arizona, USA, is one of the very few perennial rivers in the Southwest (Neary et al., 2012). It is fed by springs, flows year-round, and provides a haven for plant, animal, and human communities. Its riparian zone provides refuge for terrestrial and aquatic species including several native fish, rare reptile species, and native plant species and is also acknowledged as an “ecologically critical area” (Arizona Department of Water Resources, 1994; Neary et al., 2012; Stromberg and Stevens, 2008). Recently, however, baseflows have begun to decline (U.S. Geological Survey, 2024a, 2024b), and some research suggests that the loss in average baseflow since 2003 could be attributed to both increases in temperatures (Ellis et al., 2008), and pumping of groundwater in the upper basin (Garner et al., 2013; Pool et al., 2011). This decrease in flow and

* Corresponding author.
E-mail addresses: ltango@usgs.gov (L.L. Tango), Temuulen.Sankey@nau.edu (T.Ts. Sankey), jackson.m.leonard@usda.gov (J. Leonard), jsankey@usgs.gov (J.B. Sankey), akasprak@fortlewis.edu (A. Kasprak).

https://doi.org/10.1016/j.geomorph.2024.109231
Received 11 January 2024; Received in revised form 19 April 2024; Accepted 25 April 2024
Available online 30 April 2024

increase in temperature could potentially have negative consequences on riparian areas, native plants and animals, and allow invasive species to take over (Archer and Predick, 2008). In recent decades, the climate in the southwestern United States has become progressively more arid (Overpeck and Udall, 2020; Seager et al., 2007; Williams et al., 2020). Some models show an 85 % chance that discharge from the Verde River will be further reduced, albeit with a high level of uncertainty (Ellis et al., 2008).

Remote sensing techniques are increasingly used to detect, quantify, and improve our understanding of the Earth's geomorphic changes (Chandler, 1999; James and Robson., 2012; Lague, 2020; Lane et al., 2000; Tamminga et al., 2015; Walsh et al., 1998; Williams et al., 2012). Light detection and ranging (lidar) has emerged as an important remote sensing tool for fluvial geomorphologists (Cavalli et al., 2008; Hohenthal et al., 2011; Magirl et al., 2005; Notebaert et al., 2009). It provides more useful river assessments compared to some other historical monitoring tools because it creates data with both high spatial resolution and accuracy. Its uses include, but are not limited to, quantifying temporal changes in river channels (Kasprak et al., 2017), classifying natural surfaces (Brodu and Lague, 2012), measuring riparian vegetation roughness (Manners et al., 2013) and even tracking how energy is transferred through landscapes (Passalacqua et al., 2015). Consequently, repeat topographic data derived from lidar are useful for studying changes in river systems (Wheaton et al., 2010) at a wide range of spatial scales (Anderson, 2019).

A terrestrial laser scanner (TLS), or ground-based lidar, creates detailed and accurate data for studying fluvial geomorphology (Hohenthal et al., 2011; Notebaert et al., 2009). A TLS has high sampling density, high positional accuracy in all three spatial dimensions (X, Y, and Z) and allows for survey data to be captured in a variety of environments (Goodwin et al., 2016). Relative to other remote sensing instruments and methods, a TLS produces the most accurate geomorphic change detection results at sites with small geographic areas that are at or near sediment equilibrium (Kasprak et al., 2019); that is, a TLS can accurately quantify even very low magnitude geomorphic changes. TLS data collection has also been demonstrated to be faster and produce the best results at sites with a wide variety of geomorphic processes at work (Kasprak et al., 2019).

Here we use TLS data to characterize the riparian corridor topography and combine the high-resolution TLS data with traditional, low-resolution, transect-based measurements to quantify geomorphic changes on the UVR. U.S. Forest Service (USFS) scientists collected single line transect, laser-level topographic data in 2009, which we compare to the 2021–2022 TLS data we collected. The literature indicates that data fusion is common, but fusion between single line transect data and contemporary TLS data are rare. Other types of data fusion have been used extensively in remote sensing applications and span a wide variety of applications from forestry and river monitoring to snowpack monitoring (Donager et al., 2021; Sankey et al., 2017). For example, satellite imagery has been used in combination with bathymetry data to estimate changes between pre- and post-flooding periods (Yousefi et al., 2021). Changes in rock slopes (Ismail et al., 2022), channels after forest thinning in the wildland-urban interface (Sankey et al., 2024), snow depth and cover (Donager et al., 2021), and rivers have all been assessed using a combination of TLS, unmanned aerial vehicle (UAV)-derived photogrammetry, and hyperspectral data (Sankey et al., 2017). Additional research in riparian and fluvial environments have combined lidar, sonar, total station, aerial imagery, and RTK (Real-time Kinematic) GPS datasets (Czarnomski et al., 2011; Grams et al., 2013; Hazel et al., 2010; Kasprak et al., 2019; Solazzo et al., 2018). Urban environments, though different from the UVR, have also been monitored via data fusion between various sources of remotely sensed images (You et al., 2020). While this is not a comprehensive list of change detection methods, it illustrates that combining single line transect data with TLS data for quantitative geomorphic change detection is not extensively reported in literature. In fact, we were not able to find any published examples of single line transects being compared to TLS data for high-resolution, quantitative, geomorphic change detection.

The USFS has studied and monitored the UVR since 1993 using single line transects, focusing primarily on the conservation of native fish communities (Neary et al., 2012). The single line transects, and other similarly coarser spatial and temporal resolution plot-based data have been the primary datasets used in monitoring the UVR. For example, the single line transect data and classification of watershed conditions and channel morphology (Neary et al., 2012) using Rosgen (1994) Natural Channel Design classification system were employed to assess whether the river is geomorphically stable. A model was also developed to predict how riparian vegetation would respond to changes in river flow. The report concluded that riparian abundance – a metric defined as a function of riparian zone width, canopy foliage area, and cottonwood tree basal area – had a significant relationship to river flow; when the flow of the river decreases, so does riparian abundance. The report also concluded that changes in riparian vegetation and aquatic habitat that might lead to a change in stream classification type, are happening at too fine a scale to be measured using the Rosgen classification and recommended other sampling methods with higher spatial resolution (Neary et al., 2012). These findings have highlighted the need for accurate, precise, and high-resolution geomorphic data. The USFS is increasingly integrating real-time kinematic (RTK) survey and TLS data in their monitoring. Given the importance of the UVR, and threats posed by drought as well as groundwater and surface water withdrawals, continued monitoring is warranted, especially using TLS and RTK survey data.

Using the USFS data from 2009 and TLS data from 2021 to 2022, this study quantifies topographic changes on the UVR. Specifically, our research objectives are to:

1. characterize the riparian corridor topography and estimate geomorphic changes in elevation at established monitoring plots distributed along the UVR, and
2. account for total errors in the TLS dataset and USFS dataset in the final geomorphic change detection results.

We hypothesized that variable runoff events that have occurred since 2009 have caused statistically significant geomorphic changes to the UVR. We further hypothesized significant geomorphic changes can be quantified using data fusion between the single line transect data and contemporary TLS data.

1.1. Regional setting

The Verde River (Fig. 1) drains approximately 17,100 km^2 and flows through a narrow canyon of Paleozoic sedimentary rock and has no major perennial tributaries within the study boundaries (Arizona Department of Water Resources, 1994). The Verde River is one of only two rivers in Arizona with reaches that are federally-designated as Wild and Scenic, and is important for plant and animal communities in the natural ecosystem, as well as human communities that rely on the river water (National Wild and Scenic Rivers System, n.d.; Schenk et al., 2018). The stretch of river examined in this study is currently under review for designation as Wild and Scenic. The Verde is a unique watershed because it flows perennially and the main stem has no dams on the upper 200 km of its length (Arizona Department of Water Resources, 1994; Stromberg and Stevens, 2008). While the main stem was once dammed at the source by Sullivan dam, the springs that feed the Verde now emerge below the silted in and dry lake (Kennedy, 2023).

This study focuses on the UVR downstream of Paulden, AZ to just upstream of Sycamore Canyon, AZ. This study reach covers approximately 50 river km (Forest Service, 2010; Fig. 1). According to the Rosgen classification method (Rosgen, 1994) and the U.S. Forest Service (USFS), the UVR valley is a type IV valley, described as meandering,

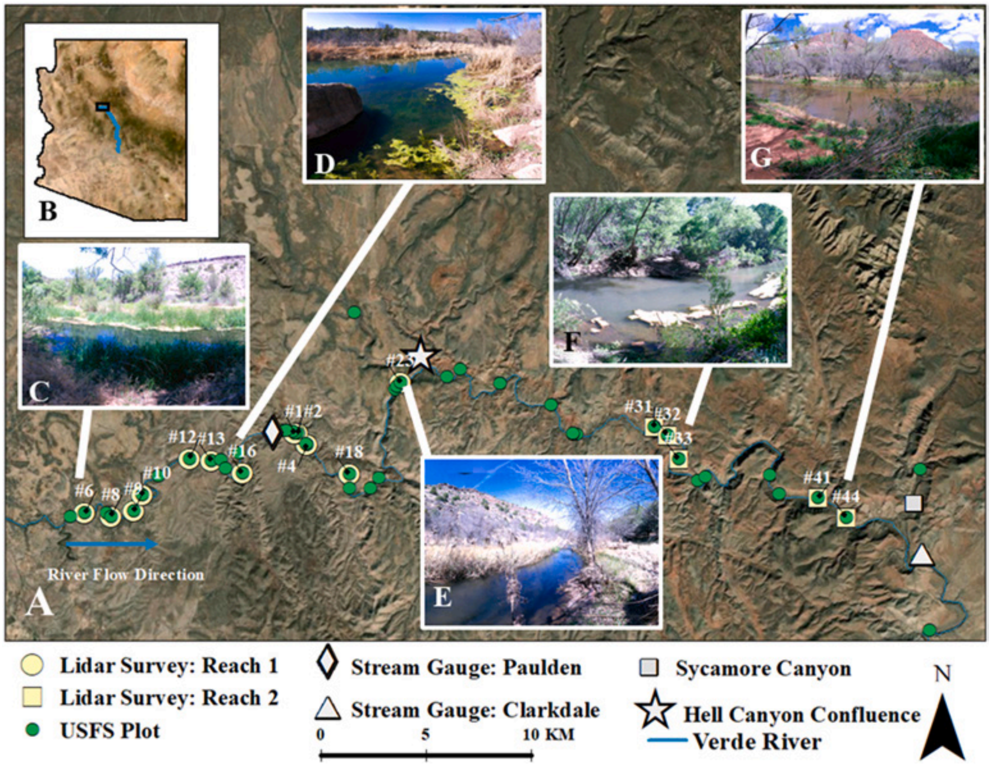

Fig. 1. The Upper Verde River study area in northern Arizona (Panel A). The location of Verde River, in blue, and the study site, outlined in black, in Arizona (Panel B). The U.S. Forest Service (USFS) has monitored a total of 40 plots since 2000 along the UVR, shown in green. Of these, we imaged 17 plots with the terrestrial lidar scanner (TLS), highlighted in yellow (Panel A), and labeled with the USFS plot numbers. Of these, plots #6, #16, #23, #33, and #44 are shown in Panels C-G respectively. Photo Credits: The basemap is from ESRI and all photographs were taken by the authors with the Leica BLK 360. (For interpretation of the references to colour in this figure legend, the reader is referred to the web version of this article.)

entrenched, and confined. The channel itself has low sinuosity and is dominated by riffles, low gradient, and generally stable banks (Neary et al., 2002). Since the character of the channel is dependent on the time since the last large flood (Stromberg and Stevens, 2008), the current megadrought in southwestern North America (Williams et al., 2020) has the potential to significantly impact geomorphology. The UVR perennial stream hydrology is controlled by both runoff and the Verde River Springs, fed by the Big and Little Chino aquifers (Stromberg and Stevens, 2008). However, baseflow is lowest in the uppermost portions of the study reach (Fries et al., 2020; Neary et al., 2012; Wirt, 2005; Wirt et al., 2000). The lowest discharges in the study area occur in plots upstream of the Hell Canyon confluence (Fig. 1).

The hydrology of the Verde River is dynamic and can be highly variable. While discharge to the UVR has significantly declined (Wirt et al., 2000), large runoff events still periodically occur (Fig. 2) (U.S. Geological Survey, 2024a, 2024b) and can cause rapid geomorphic changes across downstream landscapes (Brogan et al., 2019). The area of the watershed upstream of the stream gauge at Paulden, AZ (Fig. 2, A) is approximately 5566 km^2 and the watershed area upstream of the stream gauge at Clarkdale (Fig. 2, B) is approximately 8140 km^2. The 90th and 99th percentile discharges for the Paulden and Clarkdale gauges over the survey period, respectively, are 0.69 m^3/s, 3.2 m^3/s, and 2.51 m^3/s and 32.28 m^3/s.

The USFS established 40 plots in 2000 and sampled them via single line geomorphology transects in 2000, 2009, and 2021. Of these sampling years, we used the 2009 data to compare to terrestrial lidar data

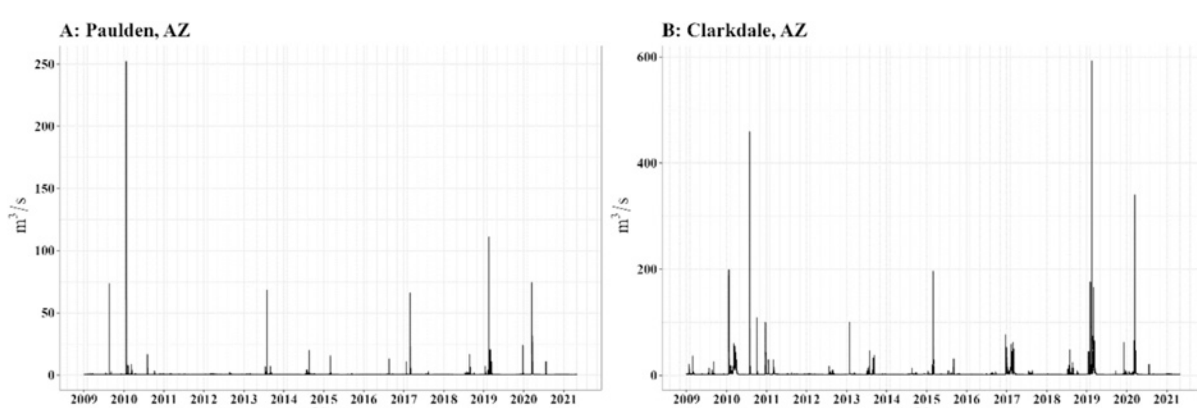

Fig. 2. USGS Stream Flow Gauge at Paulden, AZ (#09503700) (U.S. Geological Survey, 2024a, U.S. Geological Survey, 2024b) (Panel A) and at Clarkdale, AZ (# 09504000) (U.S. Geological Survey, 2024a,U.S. Geological Survey, 2024b) (Panel B) illustrating variability in UVR flow.

from 2021 to 2022. In addition to comparing the TLS data we collected in 2021–2022 to the USFS data, we also compare USFS data collected by their scientists from both 2009 and 2021 to quantify changes with data collected using a consistent field methodology. The USFS plots are distributed over the entire 50 km of the UVR from Paulden, AZ, to Sycamore Canyon, but at irregular intervals (Fig. 1). In this study, 17 of these plots were selected due to their easier access relative to other plots. Furthermore, the geomorphic setting varies along the UVR and, therefore, these plots were also chosen to encompass a variety of valley settings and reach-scale geomorphic characteristics to better understand the geomorphic changes in this watershed since 2009 (Fig. 1).

The UVR encompasses two unique reaches: Reach #1 includes the plots upstream of the Hell Canyon confluence (Fig. 1) with the main stem and Reach #2 encompasses those plots downstream of the Hell Canyon confluence. The assignments of sites to reaches was partially influenced by both the hydrology and topography of the area. While data about specific flows of tributaries is extremely sparse and there are no stream gauges in Hell Canyon, a synthesis report from 1998 concluded that Hell Canyon is a major contributor to floods on the Verde River (KIawon, 1998). We, therefore, separate our reaches at the Hell Canyon confluence.

2. Methods

2.1. Terrestrial laser scanner data

We collected TLS data, also known as lidar data, from August of 2021 to June of 2022 using the Leica BLK360 terrestrial laser scanner (TLS). Between 15 and 25 individual scans from different scan positions were acquired at each plot to cover the entire spatial extent between the north and south bank of the USFS surveys. These scans were subsequently registered and mosaicked together to create a single point cloud dataset, which was then used to create a digital elevation model (DEM) centered on the USFS single line transect location for each plot. The length, or distance between the USFS stakes on each side of the river, varied by location of each transect, but were between 30 m and 115 m among all transects. The TLS survey covered the entire length of the distance between the USFS stakes at the ends of each plot (see Data Availability statement).

The Leica BLK360 terrestrial laser scanner sends and receives a single return laser pulse centered at a wavelength of 830 nm and contains an integrated HDR digital camera that creates a 360° image by stitching together 30 individual images that are automatically spatially rectified. The vertical angle of these images is 300°. The full dome resolution of this image is 150Mp.

The laser beam diameter at the front window of the scanner is 2.25 mm with a divergence of 0.4 mrad. It has a minimum range of 0.6 m and maximum range of 60 m at 78 % albedo. Vendor-reported beam accuracies are (one sigma under the standard test conditions) 4 mm at 10 m range and 7 mm at 20 m range, and 3D point accuracy is 6 mm at 10 m range and 8 mm at 20 m range (Leica Geosystems, 2017). The high-density setting was used, which corresponds to a resolution of 5 mm at 10 m range. At this resolution, each scan took 3 min and 40 s to complete. Maximum scan rate is 360,000 points (pulses)/second. Each scan included between 30 and 60 million points.

Data preprocessing included the following steps: 1) scan-to-scan registration to create a single mosaic of each plot using CloudCompare software (CloudCompare (2.12.*2), 2021*), 2) iterative height filtering to remove all vegetation points and keep ground points only (Caster et al., 2021), 3) use the ground points to create a 10 cm resolution "bare earth" digital elevation model (DEM) (Caster et al., 2022), 4) extract elevation values from the lidar-derived DEM every 10 cm along the USFS transect line, and 5) compare the elevation of each point in the 2009 USFS data to the DEM-extracted value at that same location. Noticeably absent is georeferencing the data. Because the USFS data are not georeferenced, georeferencing was not necessary for change detection, and by omitting that step, one source of uncertainty was eliminated. However, co-registering the lidar and the USFS data together was still important. The lidar data and the USFS data were co-registered using the areas where two permanent physical rebar were present on each bank at all plots that were used by the USFS as endpoints for their single line transect. These same rebar were located in the lidar point clouds and ground points were then identified and used for co-registration. The ground point at the beginning of the transect in the USFS data was aligned with the ground point in the transect extracted from the 10 cm lidar-derived DEM. The 10 cm DEMs from all plots were compared to the USFS single line transect data.

2.1.1. Quantifying geomorphic changes and statistical significance

We derived cross-section channel data from the USFS transects and compared them to the lidar-derived DEMs. The lidar-derived DEMs were created for 17 plots over the entire 50 km of the UVR to characterize the riparian, floodplain, and upland topography for our objective #1, but the change detection analysis spans 13 years between 2009 and 2022 at only 9 plot locations, #6, #9, #10, #16, #18, #23, #33, #41, and #44 (Fig. 1) (US Forest Service, 2010). These nine plots from 2009 had comparable and detailed records among the 17 plots surveyed using the TLS. More specifically, these nine plots from 2009 were surveyed using the physical stakes present and identifiable in the field. The other 8 plots did not have any 2009 survey data associated with them. Therefore, these nine plots were the plots used for change detection between 2009 and 2021–2022, while the remaining 8 plot data were used for riparian geomorphic characterization for continued monitoring of the UVR. Additionally, lidar points in the channel were not included in any analysis because the near-infrared laser of the lidar scanner used in this survey does not penetrate through water to the channel bed; although there are other commercially available lidar scanners with different wavelength lasers that can penetrate clear water (Pratomo and Putranto, 2019).

Because there was no documentation on errors present in the USFS data, a new methodology was required to differentiate between true changes and changes that could be attributed to topographic survey errors or the inherent uncertainties of the methodologies. To do this, we assumed that the elevation of some points, specifically those furthest from the channel, had not significantly changed over the period of observation. Some of these points fall on relic terraces, and some on true hillslopes, so for the purpose of this study, they are collectively referred to as upland points. The change detection analysis involved three important steps: 1) identifying non-changing locations or upland points, 2) estimating the errors using those points as "minimum threshold errors" to differentiate between true changes vs. changes that could be attributed to errors, and 3) statistical analysis to determine whether true changes observed were significant. These steps are described in Sections 2.1.2, 2.1.3 and 2.1.4.

2.1.2. Identifying upland points

In this study, upland points, as opposed to floodplain points, were assumed to have not significantly changed over the period of observation. Consequently, they were the best proxy for zero change available in the environment. We make this assumption because over the study period no floods occurred that were large enough to reach these areas, and because the river channel and floodplain are substantially more geomorphically dynamic areas of the landscape than the upland areas that are flat or gently sloping and covered by desert vegetation. Additionally, during field observations, there was no evidence of recent geomorphic changes, or erosion at the upland points. These upland points were, therefore, used to compute the errors in comparing the lidar data and the USFS data. Identifying the upland points was a multi-step process that included the following additional datasets and tools: longitudinal slope of the channel at each plot, stream discharge, a Natural Resource Conservation Service (NRCS) cross-section analyzer (Hardy et al., 2005), and an estimate of the roughness coefficient (Manning's n).

Manning's n is an index of flow resistance needed to evaluate how friction associated with material on the banks and in the bed of a channel impact the relationship between stream discharge and stage (Coon, 1998).

Slope of the channel was determined within the spatial extent of each lidar dataset. A point at the water's surface was identified at the up and downstream ends of the channel in CloudCompare software (CloudCompare (2.12.*2), 2021*) and the change in elevation and distance between these points was determined as:

$$PercentSlope = (\Delta Z/\Delta X)^{*}100$$

Percent slope at each plot was measured by the USFS in 2021, but no documentation is available for errors in these data. Therefore, lidar-derived slope data were used for this analysis.

The second step in identifying the upland points required identifying the highest discharge that passed by each plot between 2009 and 2021. The upstream and downstream discharge data were acquired from the U. S. Geological Survey (USGS) stream gauges at Paulden, AZ (gauge #9503700) (U.S. Geological Survey, 2024a,U.S. Geological Survey, 2024b), and Clarkdale, AZ (gauge # 09504000) (U.S. Geological Survey, 2024a,U.S. Geological Survey, 2024b), respectively. Between January 2009 and May 2021, the mean discharge at the Paulden gauge was 0.73 m^3/s (26 ft^3/s) and 3.1 m^3/s (108 ft^3/s) at Clarkdale. In comparison, the mean discharge at the Paulden gauge was 1.2 m^3/s (44 ft^3/s) between 1963 and 2008 (Neary et al., 2012). These data were used to identify the largest discharge recorded during the 2009–2021 observation period. These years were chosen because they are after the period of observation for the UVR Synthesis Report (Neary et al., 2012). For Paulden, the largest discharge was 252.3 m^3/s (8910 ft^3/s) and for Clarkdale it was 591.8 m^3/s (20,900 ft^3/s). For plots #6, #9, #16, and #18, the highest discharge at the Paulden gauge was used. For the remaining plots, #10, #23, #33, #41, and #44, 283.2 m^3/s (10,000 ft^3/s) was used. The reason for this is that these were the only modeled flow we were able to locate, and a majority of the flooding that recorded at the Clarkdale gauge comes from Sycamore canyon, below the study site (KIawon, 1998).

Once slope and discharge were identified for each plot, they were entered into the NRCS Cross-section Analyzer (Hardy et al., 2005). The inputs were the USFS channel cross-section from 2009, the slope of the river section, Manning's n, and discharge. Using these inputs, the NRCS Cross-section Analyzer calculates the water surface elevation based on the geometry of the channel. Manning's n of 0.04 was used in these calculations. Any points above this flood-stage water surface elevation were labeled as upland points. These points were assumed to not have changed because none of the floods in the inter-survey period were large enough for the water to have reached the elevation of the identified upland points.

2.1.3. *Estimating error and creating error distribution*

Following delineation of upland points, we focused on quantifying errors in comparing the USFS data and the lidar-derived data without knowing the true errors in the historical USFS data. Quality of historical topographic data are usually the limiting factor in accurately assessing geomorphic changes (James et al., 2012). In this study, the traditional USFS data are a limiting factor, whereas the lidar data have a vendor-reported accuracy of 5 mm with a 360^0 field of view. Not only does the USFS data create a single line channel cross-section, but the cross-section data also has low spatial resolution compared to the lidar data. The USFS single line transect measurements have between 20 and 40 points per 40 m to 100 m lengths.

An Empirical Cumulative Distribution Function (ECDF) (R Core Team, 2023) was used to determine the probability of a "true" change at each point. Using the upland data from 2009 USFS data and the 2021 lidar data, a cumulative probability distribution of errors between the datasets was created using the ECDF (Fig. 3, B). Comparing 2021 USFS data collected by USFS scientists and 2021 lidar data we collected would be an alternate way to determine true change, but we chose to use 2009 USFS data and 2021 lidar data we collected to minimize compounding errors. The ECDF was then used to create an empirical *p*-value for the probability that an observed topographic change at each point is a 'true' change vs. a change that could be explained by the error distribution in the upland points. If a change had an empirical p-value of <0.05, the change was considered true change. The error distribution, with a mean of −0.06 m, was not centered on zero (Fig. 3, A). Even with this small deposition bias, these upland points are best points to use for error distribution analysis.

2.1.4. *T-tests and bootstrapping*

To determine if the changes observed in Reach #1 were significantly different compared to the changes observed in Reach #2, both difference in means *t*-tests and bootstrapping were used. t-tests were used to compare: 1) mean of the observed changes in Reach #1 compared to Reach #2, and 2) the positive changes, or sediment deposition, in Reach #1 compared to the positive changes in Reach #2. An additional method, bootstrapping, was used to verify the results of the t-test. Bootstrapping consists of randomly sampling the entire dataset multiple times to simulate many different data populations. In this case, each population was sampled 1000 times to create a new simulated 'mean' for the data. Other questions could be answered using these methods, but this analysis was constrained to examine how the reaches compare to one another, and not what geomorphic processes were responsible for the differences between each reach.

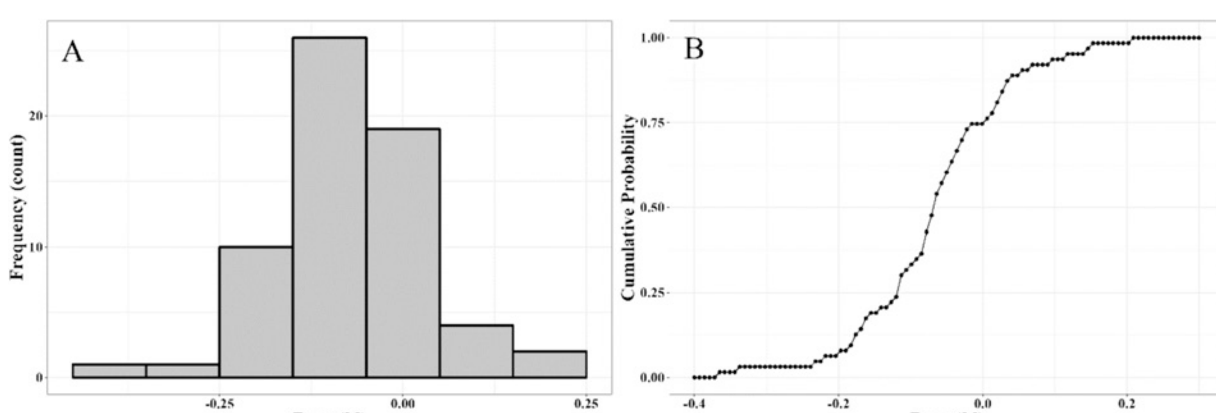

Fig. 3. The distribution of errors in the upland points between the 2009 USFS data and the 2021 lidar data (Panel A). The cumulative probability of each error occurring in the upland point comparison dataset (Panel B).

2.2. USFS data–derived geomorphic change and statistical significance

The USFS has consistently used single line transects to monitor the UVR (Neary et al., 2012). To identify a channel cross-section, stakes were installed on both north and south banks of the channel with a measuring tape stretched between the two stakes. Using a laser level, the vertical distance from the tape to the ground was measured along the tape. Starting on the north bank of each plot, the vertical distances were measured at typically 1-5 m horizontal intervals to create a single line cross-section of the channel geometry. Using this process allows a channel cross-section to be derived using simple equipment with minimal effort (Ray and Megahan, 1979). We also compared USFS data from 2009 and 2021 ($N = 9$ plots) to detect changes within this dataset alone. The same methodology as described above was used in this comparison with one notable exception. Distance intervals between points were different in the 2021 survey than those from the 2009 survey. To create points at the same distance intervals for both years, the R software package, Zoo (R Core Team, 2023; Zeileis and Grothendieck, 2005) was used to interpolate points along the transect using distance as weight. After these points were created, we examined the changes in elevation (Z dimension). The Zoo package uses the distance between the closest known point in both datasets, and the distance between that point and the next known point to interpolate what the new point value will be. For example, if the Z value of a point at 1 m along the X axis is 1 m and the Z value of a point at 2 m along the X-axis is 2 m, the Z value of a point at 1.2 m would be interpolated to 1.2 m. Upland points or non-changing points were also identified as described above.

3. Results

3.1. Lidar and USFS data comparison

A total of 17 plots were surveyed with the TLS, and we successfully generated detailed DEMs at all plots to characterize the riparian, and upland zone topography for continued monitoring. Each plot was scanned with 15–25 scans from different scan position locations. The individual scans at each plot were all successfully registered together to create a full image of the area. The mean RMSE of scan-to-scan registration at each site was 0.024 m.

Only 9 of the 17 plots were used for change detection. Topographic data from the 2009 USFS survey were compared to the 2021–2022 lidar data for the geomorphic change detection (Table 1).

The results indicated that there were statistically significant changes at all 9 plots available for comparison (Fig. 4). Based on our methods of identifying statistically significant changes, there were also changes that we could attribute only to errors at all 9 plots (Fig. 5). These changes are not volumetric changes and are not intended to be extrapolated to volume. Instead, they represent changes in the elevation of individual points along each single line transect. The average p-value for the significant changes was 0.01. Other than Plot #16, more deposition than erosion occurred at all plots, and the vertical magnitude of most of the changes, whether deposition or erosion, ranged between 1 cm and 50 cm. The deposition predominantly occurred in the floodplain nearest the channels. Most of the statistically significant changes occurred near the channel. The notable exception was Plot #16, which eroded on the south bank further away from the channel. Overall, the USFS data and lidar data comparison supported the hypothesis that significant geomorphic changes can be quantified using data fusion between the two data types.

Results indicate that significant geomorphic changes have occurred along the entire 50 km length of the UVR. It is important to explore if there is a difference between trends in the upper reach in comparison to the lower reach because there is a watershed boundary and it is the major tributary to the Verde River along the study reach (KIawon, 1998; Neary et al., 2012). The change detection results indicate that Reach #2 changed significantly (p-value $= 0.05$) more compared to Reach #1 since 2009. Specifically, there has been more deposition in Reach #2 than in Reach #1 (p-value = 0.014). Bootstrapping further supported these results by showing that: 1) approximately 98.2 % of the bootstrapped mean value of changes in Reach #2 are greater than mean value of the changes in Reach #1, and 2) approximately 86.5 % of the bootstrapped depositional changes in Reach #2 are greater than the mean depositional changes in Reach #1.

3.2. USFS data comparison

Topographic data from the 2009 USFS laser-level survey were compared to the 2021 USFS laser-level survey for geomorphic change detection (Table 2). Importantly, the results were consistent with the change detection results from the comparison between the 2009 USFS survey and the 2021 lidar survey (Figs. 6 and 7). These topographic changes are not intended to be extrapolated to a volume or mass of change in sediment storage. They represent changes in the elevation of individual points along each single line transect. First, consistent with the lidar-derived results, the USFS analysis results indicate that most of the changes occurred near the channel and were consistently depositional (Fig. 7). Notable exceptions are Plots #44 and #10. Plot #44 was not used in any analysis due to the 2009 and 2021 topographic surveys not being in the same geographical location, which inaccurately indicates more change than actually occurred. The same issue is present at Plot #10, although the error is smaller compared to Plot #44. Secondly, consistent with the lidar results, the USFS data comparison indicate that Reach #2 changed significantly more compared to Reach #1 (Table 2). Specifically, the USFS data comparison indicate that significantly more deposition occurred in Reach #2 than in Reach #1. Thirdly, the t-tests indicate that mean changes are also moderately significantly different between the two reaches (significance level of 0.1): Reach #2 has changed significantly more than Reach #1 (p-value = 0.09). An additional t-test showed that not only are the means statistically different, but the mean deposition in Reach #2 is greater than the mean deposition in Reach #1 (p-value = 0.056). Also, the average p-value for significant changes was 0.03.

4. Discussion

This study documented several important findings. First, we developed a new data fusion technique that integrates traditional line transect-based measurements with lidar survey and statistical analysis to estimate and identify significant geomorphic changes. Secondly, we

Table 1
Summary of lidar-derived plot data and geomorphic change detection results using 2009 USFS data and 2021 lidar data. Mean values do not include non-significant or 0 change.

	Lidar-derived plot data summary				Change detection summary from 2009 USFS data and 2021 lidar data				
Reach	Mean Channel Width	Mean Plot Length	Mean Plot Width	Relief	Mean Vert. Change	Max Deposition	Max Erosion	Mean RMSE	Mean P-Value
Reach 1	17.2 m	55 m	79 m	7.2 m	+0.21 m	+0.91 m	−0.37 m	0.024 m	0.014
Reach 2	13.5 m	47 m	86 m	6.0 m	+0.30 m	+0.97 m	−0.36 m	0.024 m	0.013
Combined Reaches	15.4 m	51 m	83 m	6.6 m	+0.30 m	+0.97 m	−0.37 m	0.024 m	0.014

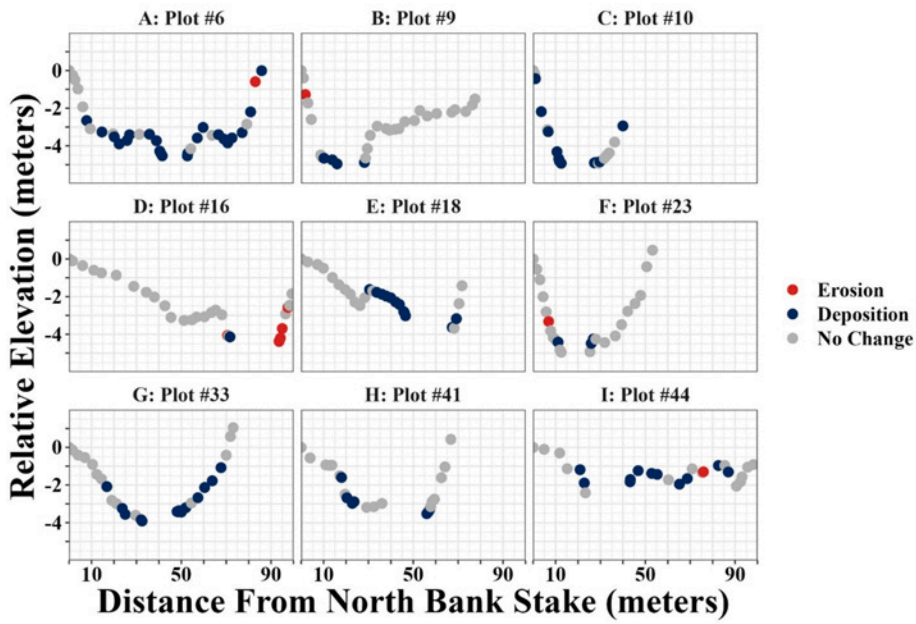

Fig. 4. Lidar-derived change detection results and channel cross-sections showing where significant changes occurred. Points are colored by whether they represent positive topographic change interpreted as sediment deposition, negative topographic change interpreted as erosion, or no change. Channel cross sections created from the 2021 lidar data in panels A – F are plots in Reach #1. Panels G – I are plots in Reach #2.

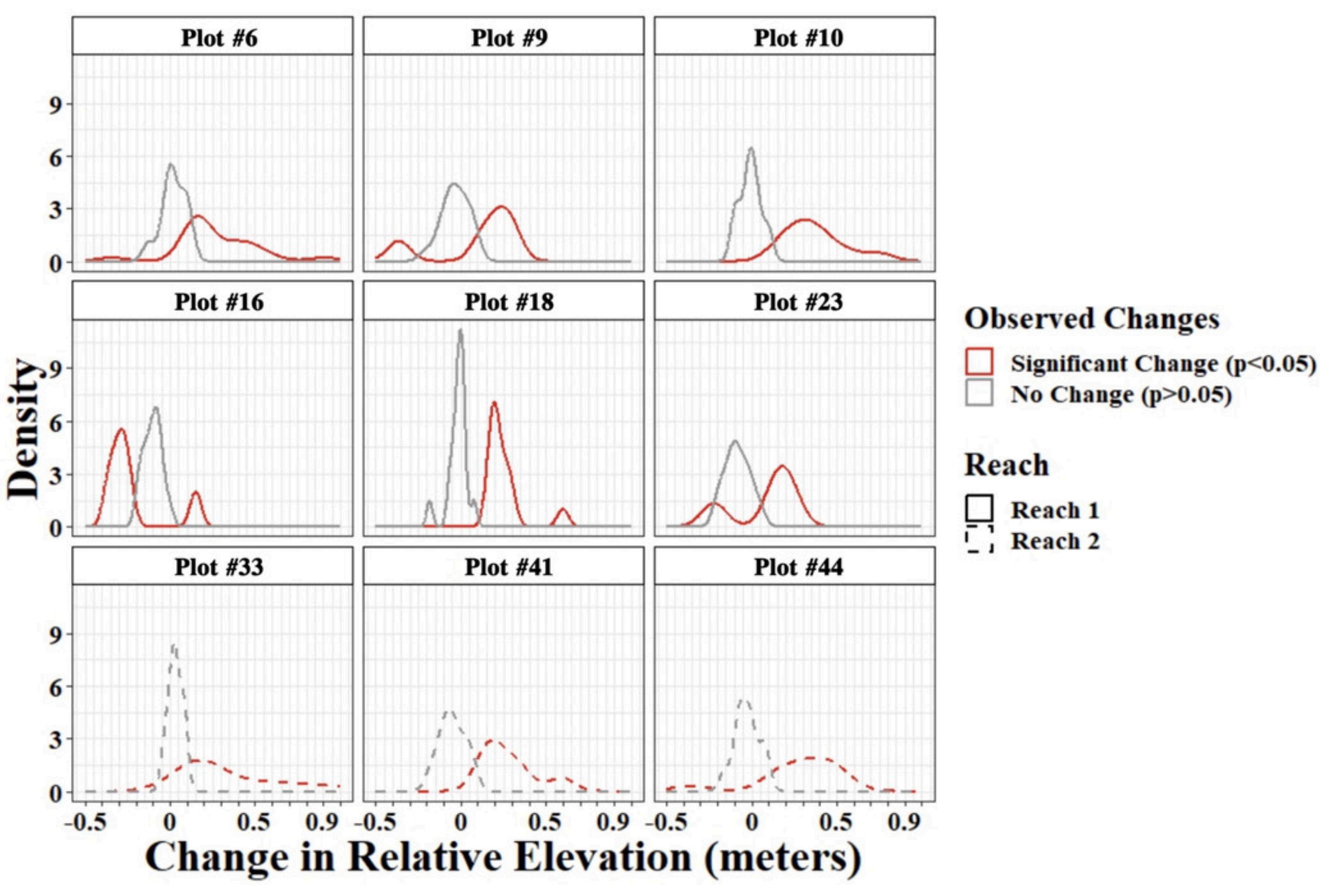

Fig. 5. Lidar-derived change detection results. Density plots that indicate the proportion of points along the cross-section that had observed changes of elevation indicated on the X-axis. Gray lines represent non-significant changes, while red represents significant, or true, changes. (For interpretation of the references to colour in this figure legend, the reader is referred to the web version of this article.)

Table 2
Summary of USFS data from 2009 and geomorphic change detection results between 2009 USFS data and 2021 USFS data. Plot #44 was not included in these data. Mean values do not include non-significant or 0 change.

	USFS-derived plot data summary			Change detection summary from 2009 USFS data and 2021 USFS data		
Reach	Mean Channel Width	Mean Bankfull Width	Mean Bankfull Depth	Mean Vert. Change	Max Deposition	Max Erosion
Reach 1	15.6 m	14.3 m	1.1 m	+0.03 m	+1.25 m	−0.73 m
Reach 2	15.7 m	16.4 m	1 m	+0.06 m	+1.16 m	−0.54 m
Combined Reaches	15.7 m	15.4 m	1.1 m	+0.04 m	+1.25 m	−0.73 m

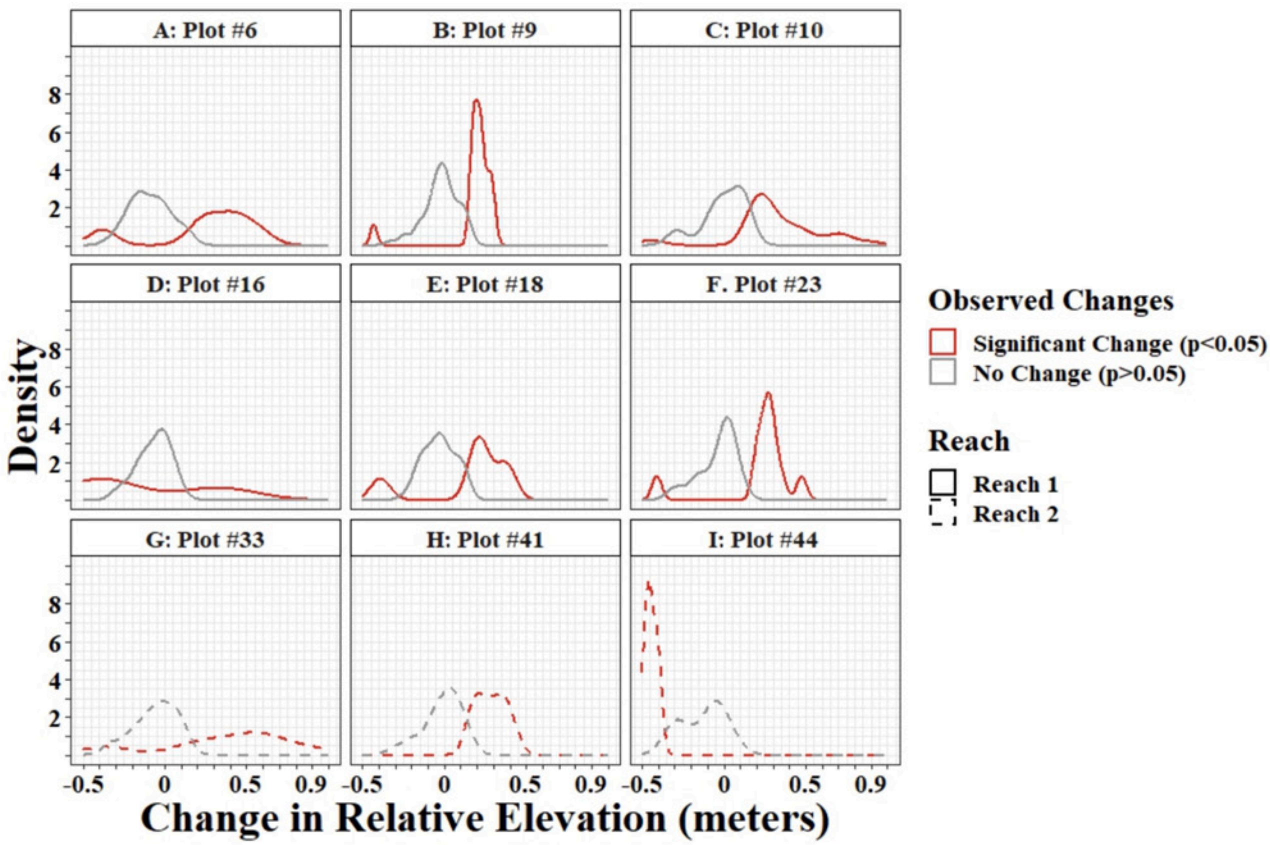

Fig. 6. USFS data-derived density results. Density plots indicate the proportion of points along the cross-section that had observed changes of elevation indicated on the X-axis. Gray lines represent non-significant changes, while red represents significant, or true, changes (p-value $\leq$0.05). (For interpretation of the references to colour in this figure legend, the reader is referred to the web version of this article.)

documented that statistically significant geomorphic changes occurred along the UVR between 2009 and 2021–2022. Several different geomorphic processes might have contributed to the observed changes in this ecosystem. These findings are discussed below along with management implications.

4.1. New methodology

This study combined traditional transect-based measurements from the USFS with contemporary lidar data that we collected to detect geomorphic changes along the UVR (Fig. 8). Specifically, two-dimensional single line transect data in relatively coarse spatial resolution from the USFS was combined with three-dimensional (3D), high resolution TLS data we collected in 2021–2022. This integration required the contemporary 3D data to be coarsened in spatial resolution and spatially subset to match the USFS dataset. In doing so, this study established a quantitative and statistically sound methodology to fuse these types of data. This workflow is important because it paves the way for a new type of data fusion analysis with statistical analysis of significant changes; using this approach might help land management agencies obtain accurate information about the UVR. This method can be used in other river systems, where single line cross section data have been collected and where TLS data can be collected.

In comparing the USFS data with the contemporary TLS data, we used a combination of GIS and statistical analysis tools to ensure that changes observed were true changes, rather than changes that could be attributed to errors in the datasets. Since the USFS did not report errors associated with their data, we instead used a statistical approach to create a true change curve. Specifically, each point in the dataset was compared to a modeled error curve to estimate, based on points that were assumed to not have changed, a probability of significant "true" change (p-value <0.05). This resulted in quantitative change detection results with statistical significance, which can be used to make more reliable inferences. Furthermore, comparing single line transect data to lidar data resulted in greater detection of geomorphic changes compared to transect data alone. Statistically significant changes made up 38 % of the changes detected when using the USFS transect data and lidar data. When using only the USFS transect data, only 20 % of the detected changes were statistically significant. Importantly, the change detection results were consistent between both methods. However, since the

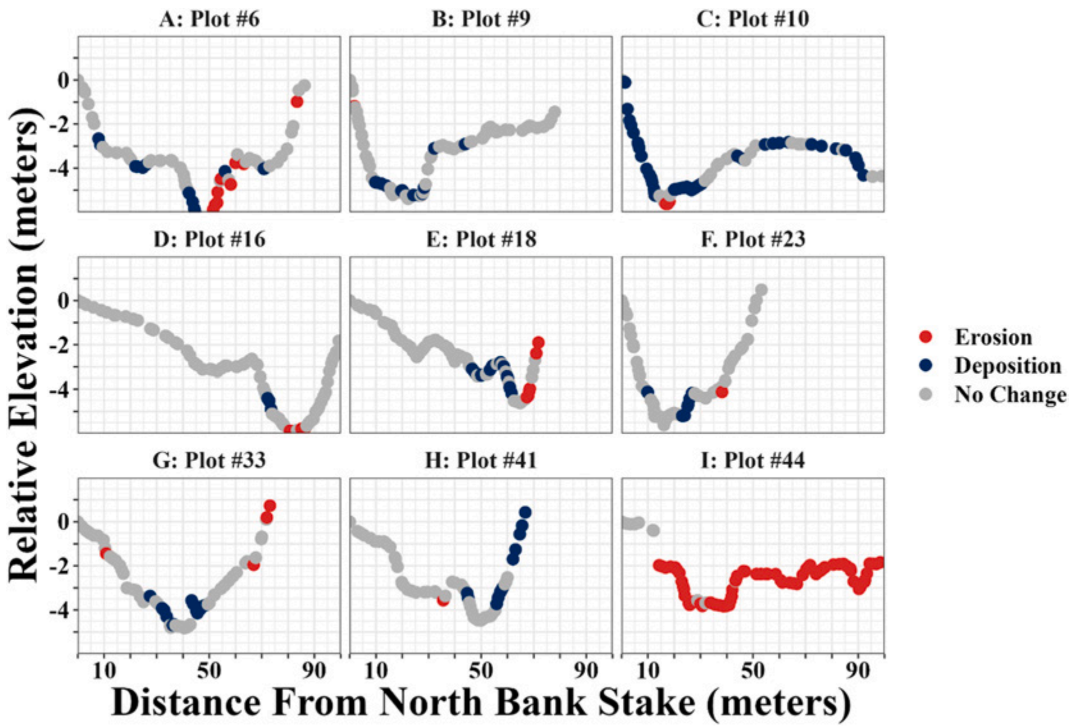

Fig. 7. USFS data-derived change detection results. Channel cross-sections are shown highlighting where the significant changes occurred, colored by whether they are deposition or erosion. Panels A – F are plots in Reach #1. Panels G – I are plots in Reach #2.

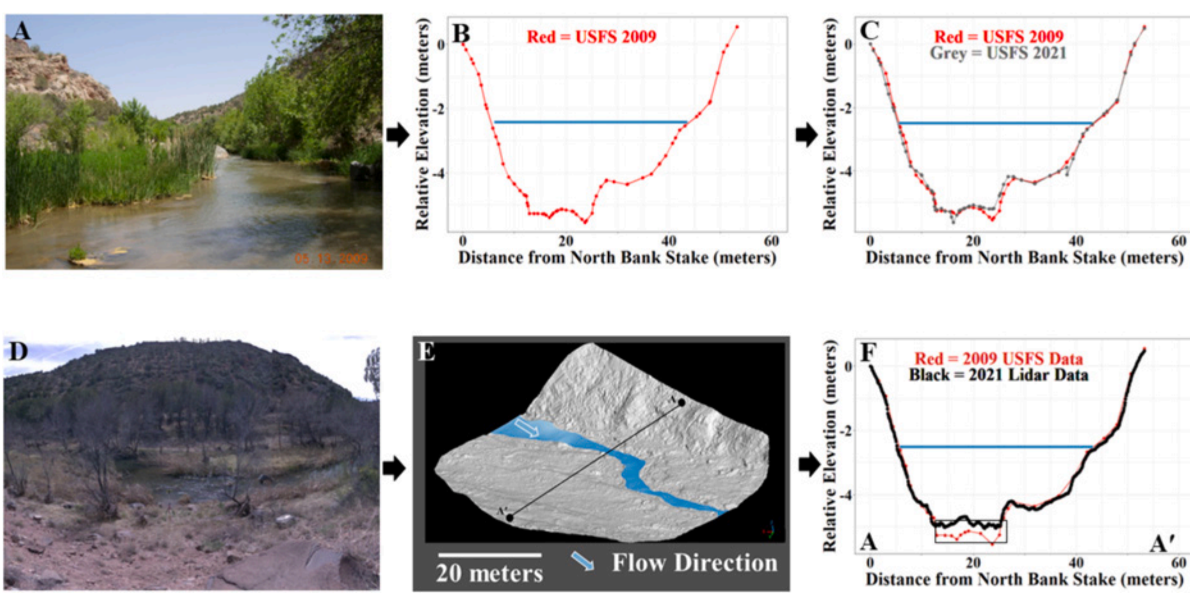

Fig. 8. Illustration of the datasets, their integration, and results at plot #23. An image taken by a USFS scientist looking downstream with the north bank on the left in 2009 (Panel A) and an image we collected using the TLS from the north bank looking south in 2021 (Panel D). Cross sections derived from USFS data showing 2009 (Panel B) data and the 2009 and 2021 data (Panel C). Lidar-derived DEM (Panel E) showing where the USFS cross section is located, and the upland points are at the ends of the cross section marked with A (Panel E). Cross section showing 2009 USFS data with the lidar-derived cross section data (Panel F). The black box indicates where lidar data were not usable due to the lidar sensor not capturing information below water. The blue line in panels B, C, and F indicate modeled high-water mark for the survey interval. All points above it were considered upland points for analysis purposes. (For interpretation of the references to colour in this figure legend, the reader is referred to the web version of this article.)

average p-value was lower for lidar-derived change detection results, statistically, we can be more certain of results using the lidar-based methodology.

The new method that was developed and successfully implemented in this study also provides an important bridge between legacy data and modern topographic surveying technologies used in a range of scientific applications. These techniques also diverge in their level of user technical expertise. Single line transects are used in many different natural resource monitoring applications (U.S. National Park Service, 2021), including stream and watershed health surveys (Neary et al., 2002; U.S. Geological Survey, 1998) and vegetation biomass measurements (Marshall et al., 2000; Van Deusen and Gove, 2011). Increasingly, however, the TLS is being used to monitor these same natural resources (Day et al., 2013; Heathfield et al., 2016; Kasprak et al., 2019). Still, change detection is limited to data collected in recent time periods since the new technology only recently became available for repeated measurements. Traditional line transect data, especially the older historical datasets, have not been commonly leveraged in change detection studies with recent TLS-based measurements. Although there are studies assessing geomorphic changes using aerial lidar and channel cross sections (Major et al., 2019), we are using terrestrial lidar at much finer scale and higher spatial resolution. The new method demonstrated in this study will be invaluable in bridging the gap between the times where agencies and researchers used traditional methods and when newer and better technology become available.

4.2. Geomorphic changes

Our results indicate that important geomorphic changes have occurred over the last 13 years along the UVR. Specifically, significant sediment deposition has occurred along the UVR floodplain since 2009. Research along rivers in the western United States has shown that floodplain development is associated with flow duration, frequency, and vegetation establishment (Merritt, 2022). In periods of lower river flows, floodplain accretion is associated with increases in bank vegetation (Merritt, 2022). The plots surveyed in this study since 2009 have experienced a mean deposition or average vertical change of +0.3 m. Our study period from 2009 to 2021, in general, has been a period of relative stability. Our results indicate that small to medium-sized flows have likely deposited sediment near the channel, which is consistent with the literature that deposition is commonly occurring along other rivers in the southwestern United States. For example, vertical floodplain accretion occurred on the Little Colorado River in the 1970s during a period of decreased discharge. The floods that occurred in the period of lower discharge were responsible for sediment deposition on the floodplain (Hereford, 1984). A more recent study of the Little Colorado River concluded that the total annual flow and annual peak flow showed negative trends between 1996 and 2016 that coincided with channel narrowing and vertical aggradation of the floodplain (Dean and Topping, 2019).

In addition to the periodic, large flood events (Fig. 2), several potential factors could contribute to the changes observed in this study: 1) decreased average river flow (Fig. 9), 2) vegetation encroaching into the channel, and 3) increase in bankfull depth. Although large flood events have occurred, average discharge of the UVR between Paulden, AZ, and Sycamore Canyon has decreased over the last 13 years (Fig. 9) (U.S. Geological Survey, 2024a, 2024b).

The U.S. Geological Survey (USGS) gauge data indicate that the average discharge of the UVR at the Paulden, AZ, gauge decreased from 1.2 m^3/s (44 ft^3/s) between 1963 and 2008 to 0.73 m^3/s (26 ft^3/s) between 2009 and 2021 (U.S. Geological Survey, 2024a, 2024b). This could be due to the current warming trends that have already caused irreversible damage to the resilience and extent of freshwater ecosystems in some parts of the world beyond a point where they can adapt quickly enough (Pörtner et al., 2022). In other words, these ecosystems are changing so quickly, and the organisms and environmental processes do not have time to adjust to the new climate, therefore causing damage that is not repairable. Some rivers in the southwestern United States are predicted to continue to have a reduction in flows over the coming decades (Archer and Predick, 2008; Ellis et al., 2008; Overpeck and Udall, 2020; Salehabadi et al., 2022), and the consequences of those reductions are unlikely to be naturally reversed. Such reductions in flow can lead to vegetation encroachment from both a lack of large scouring flood events (Dean and Topping, 2019; Grams et al., 2020) and a possible dewatering of wet streamside areas at higher river stage elevations that allows for woody vegetation expansion into the channel towards lower river stage elevations (Sankey et al., 2015). Flow reductions can also lead to changes in the channel shape and size and contribute to the floodplain deposition (Cadol et al., 2011). An increase in vegetation can further promote the deposition of sediment along river (Merritt, 2022). Consistent with patterns observed in other rivers on the Colorado Plateau, dense vegetation was observed along the UVR in both Reach #1 and Reach #2 (Fig. 1). Vegetation plays an important role in sediment deposition in fluvial environments (Marjoribanks et al., 2019) by reducing flow velocity, increasing bank stability, and increasing roughness and drag to promote sediment deposition (Dean and Topping, 2019; Grams et al., 2020). A decrease in discharge allows vegetation to establish in the channel. Subsequent smaller floods, in turn, deposit sediment in the established vegetation (Cadol et al., 2011), leaving it trapped when the water recedes. With fewer large floods to clear the system, vegetation can grow and flourish and, therefore, alter channel morphology by giving cohesion to banks (Merritt, 2022; Wenger, 1999) and altering sediment delivery (Cadol et al., 2011). Molina et al. (2009) further illustrate that vegetation is the most important factor for short-term sediment deposition (Molina et al., 2009). Along the UVR, invasive cattails were commonly observed on the banks of the channel (Figs. 8 and 10), which might contribute to the observed sediment deposition.

Average bankfull depth in 2009 at the plots used in this study was recorded to be under 0.8 m (Neary et al., 2012), whereas average bankfull depth in the 2021–2022 USFS survey was 1.12 m. However, over our study interval, the average vertical distance between the north bank stakes and the channel bed has not increased, demonstrating that the channel bed is not at a lower elevation in 2021 than it was in 2009, although the USFS data are not georeferenced. This finding could indicate that the channel bed is being scoured and lowering in elevation or

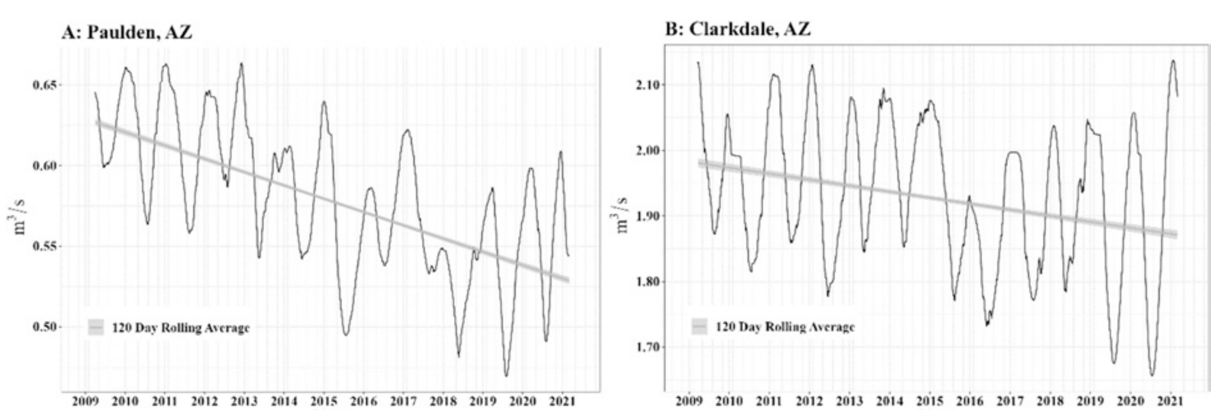

Fig. 9. The 90th percentile average daily discharge at Paulden, AZ (#09503700, Panel A) (U.S. Geological Survey, 2024a, 2024b) and Clarkdale, AZ (# 09504000, Panel B) (U.S. Geological Survey, 2024a, 2024b) showing an overall decrease in discharge over the study interval.

Fig. 10. Photographs taken by a USFS technician from 2009 (Panel A) and 2021 (Panel B) at Plot #1 illustrating the changes in channel width and cattail density over the study period.

incising, although lidar data cannot detect this for portions of the channel that were inundated by water when the data were acquired in this study. However, since our change detection results conclusively demonstrate that deposition has occurred in the floodplains, the increase in bankfull depth is likely a product of the floodplain increasing in elevation, or aggrading, rather than channel incision. This interpretation is also consistent with the patterns of increased vegetation and reduced flow of the UVR.

Decrease in flow, whether by upstream diversion, groundwater pumping, or drying can lead to disconnection of the channel from the floodplain. Channelization is a characteristic of this disconnection (Grams et al., 2022; Hauer and Lorang, 2004; Wohl, 2005). Because the deposition occurred near to the channel (Figs. 4 and 7), the channel of the UVR appears to be disconnecting from the floodplain. River systems in the southwestern United States are not as dynamic as they once were, and drying is associated with changes in riparian vegetation, decrease in plant biodiversity, habitat degradation, and a departure from the natural processes in the floodplain (Hauer and Lorang, 2004; Stromberg et al., 2007). The results of this study suggest that some of these factors might be at work in the UVR.

4.3. Management implications of repeat TLS survey

We note that the TLS data collected in this study will provide an important high-resolution baseline dataset for the UVR system, although this study was limited by the spatial resolution of the USFS single line transect data. The TLS instrument used in this study has a vendor-reported accuracy of (one sigma under the standard test conditions) 5 mm at 10 m range and each scan included between 30 and 60 million laser points. Future studies on the UVR could collect similar TLS data with the same spatial resolution and accuracy to continuously monitor the river system and detect changes in three dimensions. Comparing repeat TLS data acquisitions will provide unprecedented accuracy in assessing geomorphic changes that include sediment volumes, vegetation density, and channel changes within the survey boundaries (Lague, 2020; Sankey et al., 2024; Wheaton et al., 2010). Repeat TLS data can also be used to assess sediment capture by plants in fluvial environments by analyzing sediment changes near and around vegetation patches, although attaining these results is complex and includes preprocessing and filtering the data (Marjoribanks et al., 2019). Quantifying sediment capture with repeat topographic survey along the UVR could help us better understand the role of vegetation, or channel narrowing.

Quantifying changes and identifying specific locations of the changes will be invaluable to managers as they face a changing and drying world. UVR hydrology is at risk due to the current megadrought in the American Southwest (Williams et al., 2020). Rivers in the region are predicted to get drier due to reductions in flow caused by climate change and subsequent aridification (Overpeck and Udall, 2020). Consequently, the loss of flow in the UVR can have far-reaching consequences to the plants and animals that depend on the riparian habitat (Archer and Predick, 2008). Given the quantitative change detection results from the last 13 years, continued repeat TLS surveys will be invaluable to managing the UVR for the future. It not only gives insight into how the habitat might be changing, but what geomorphic processes might be driving those changes.

5. Conclusion

The new method used in this study demonstrates that quantitative change detection is possible by comparing traditional single line transect data to contemporary TLS data. Our results indicate that there have been significant topographic changes since 2009 along the UVR, and those changes have been overwhelmingly aggradation due to sediment deposition. Given that the mean discharge of the river between 2009 and 2021 is lower than between 1963 and 2008, the observed geomorphic changes might be associated with the decrease in mean discharge and vegetation encroachment throughout the corridor, though other research would be needed to confirm this. While there has been variability in stream flow between 2009 and 2021, the trend is moving towards lower discharges (Fig. 9) (U.S. Geological Survey, 2024a, 2024b). The method demonstrated in this study provides an important bridge between traditional, field-based methods and new technology, and provides managers with a new tool to assess how river corridors are responding to changing climate.

CRediT authorship contribution statement

Lauren L. Tango: Writing – original draft, Visualization, Methodology, Formal analysis. **Temuulen Ts. Sankey:** Conceptualization. **Jackson Leonard:** Funding acquisition, Conceptualization. **Joel B. Sankey:** Writing – review & editing, Conceptualization. **Alan Kasprak:** Writing – review & editing, Conceptualization.

Declaration of competing interest

The authors declare that they have no known competing financial interests or personal relationships that could have appeared to influence the work reported in this paper.

Data availability

Data are not currently available from the funding organizations, the U.S. Bureau of Reclamation, and the U.S. Forest Service. Contact the U.S. Bureau of Reclamation or the U.S. Forest Service for further information.

Acknowledgements

We would like to thank members of the Remote Sensing and Geoinformatics lab at Northern Arizona University for their input and assistance. Joshua Caster, of the U.S. Geological Survey (USGS), has been invaluable for all his incredible guidance and support as the expert in all things lidar. Blase Lasala has also helped assist with lidar research and exploring alternate software and scan registration techniques. We would also like to send a huge thank-you to Wade Gibson, without whom fieldwork would not have been done in a timely manner. Thank you to the funding agencies, the U.S. Bureau of Reclamation, the U.S. Forest Service (21-JV-11221634-053), and Northern Arizona University. Joel B. Sankey was supported by the USGS Ecosystems Mission Area. This manuscript is submitted for publication with the understanding that the U.S. Government is authorized to reproduce and distribute reprints for Governmental purposes. Any use of trade, product, or firm names is for descriptive purposes only and does not imply endorsement by the U.S. Government.

References

Anderson, S.W., 2019. Uncertainty in quantitative analyses of topographic change: Error propagation and the role of thresholding. Earth Surf. Process. Landf. 44 (5), 1015–1033. https://doi.org/10.1002/ESP.4551.

Archer, S.R., Predick, K.I., 2008. Climate Change and Ecosystems of the Southwestern United States. Society for Range Management. https://bioone.org/journals/Rangelands/volume-30/issue-3/1551-501X(2008)30[23:CCAEOT]2.0.CO;2/Climate-Change-and-Ecosystems-of-the-Southwestern-United-States/10.2111/1551-501X(2008)30[23:CCAEOT]2.0.CO;2.full.

Arizona Department of Water Resources, 1994. Arizona Riparian Protection Program Legislative Report.

Brodu, N., Lague, D., 2012. 3D terrestrial lidar data classification of complex natural scenes using a multi-scale dimensionality criterion: applications in geomorphology. ISPRS J. Photogramm. Remote Sens. 68 (1), 121–134. https://doi.org/10.1016/J.ISPRSJPRS.2012.01.006.

Brogan, D.J., Nelson, P.A., MacDonald, L.H., 2019. Spatial and temporal patterns of sediment storage and erosion following a wildfire and extreme flood. Earth Surf. Dyn. 7 (2), 563–590. https://doi.org/10.5194/ESURF-7-563-2019.

Cadol, D., Rathburn, S.L., Cooper, D.J., 2011. Aerial photographic analysis of channel narrowing and vegetation expansion in Canyon De Chelly National Monument, Arizona, USA, 1935-2004. River Res. Appl. 27 (7), 841–856. https://doi.org/10.1002/rra.1399.

Caster, J., Sankey, T.Ts., Sankey, J.B., Bowker, M.A., Buscombe, D., Duniway, M.C., Barger, N., Faist, A., Joyal, T., 2021. Biocrust and the soil surface: Influence of climate, disturbance, and biocrust recovery on soil surface roughness. Geoderma 403, 115369. https://doi.org/10.1016/j.geoderma.2021.115369.

Caster, J., Sankey, J. B., Fairley, H., & Kasprak, A. (2022). Terrestrial lidar monitoring of the effects of Glen Canyon Dam operations on the geomorphic condition of archaeological sites in Grand Canyon National Park, 2010–2020. In *Open-File Report* (2022–1097). U.S. Geological Survey. doi:https://doi.org/10.3133/ofr20221097.

Cavalli, M., Tarolli, P., Marchi, L., Dalla Fontana, G., 2008. The effectiveness of airborne LiDAR data in the recognition of channel-bed morphology. CATENA 73 (3), 249–260. https://doi.org/10.1016/j.catena.2007.11.001.

Chandler, J., 1999. Effective application of automated digital photogrammetry for geomorphological research. Earth Surf. Process. Landf. 24 (1), 51–63. https://doi.org/10.1002/(SICI)1096-9837(199901)24:1<51::AID-ESP948>3.0.CO;2-H.

CloudCompare (2.12.2), 2021 [Computer software]. http://www.cloudcompare.org/.

Coon, W.F., 1998. Estimation of Roughness Coefficients for Natural Stream Channels with Vegetated Banks. US Geological Survey. https://play.google.com/books/reader?id=viUnx0wDvL4C&pg=GBS.PR10&hl=en.

Czarnomski, N., Wheaton, J., Grams, P., Hazel, J., Kaplinski, M., Schmidt, J., 2011. Untangling Geomorphic Processes in the Grand Canyon with Topographic Time Series from Hybrid Surveys. 1322.

Day, S.S., Gran, K.B., Belmont, P., Wawrzyniec, T., 2013. Measuring bluff erosion part 1: Terrestrial laser scanning methods for change detection. Earth Surf. Process. Landf. 38 (10), 1055–1067. https://doi.org/10.1002/esp.3353.

Dean, D.J., Topping, D.J., 2019. Geomorphic change and biogeomorphic feedbacks in a dryland river: the Little Colorado River, Arizona, USA. GSA Bull. 131 (11−12), 1920–1942. https://doi.org/10.1130/B35047.1.

Donager, J., Sankey, T.Ts., Sánchez-Meador, A., Sankey, J.B., Springer, A., 2021. Integrating airborne and mobile lidar data with UAV photogrammetry for rapid assessment of changing forest snow depth and cover. Science of Remote Sensing 4, 100029. https://doi.org/10.1016/J.SRS.2021.100029.

East, A.E., Sankey, J.B., 2020. Geomorphic and Sedimentary Effects of Modern climate Change: current and anticipated Future Conditions in the Western United States. Rev. Geophys. 58 (4), e2019RG000692 https://doi.org/10.1029/2019RG000692.

Ellis, A.W., Hawkins, T.W., Balling, R.C., Gober, P., 2008. Estimating future runoff levels for a semi-arid fluvial system in Central Arizona, USA. Climate Res. 35 (3), 227–239. https://doi.org/10.3354/CR00727.

Forest Service, 2010. Upper Verde River Eligibility Report Update for the National Wild and Scenic River System: Prescott National Forest. https://www.fs.usda.gov/Internet/FSE_DOCUMENTS/stelprdb5342134.pdf.

Fries, A., Wilson, M., Steele, N.L.C., 2020. Verde River Watershed Report Card Friends of the Verde (March).

Garner, B., Pool, D.R., Tillman, Fred D., & Forbes, Brandon T. (2013). Human effects on the hydrologic system of the Verde Valley, Central Arizona, 1910–2005 and 2005–2110, using a regional groundwater flow model. U.S. Geological Survey Scientific Investigations Report 2013–5029. 47 p. https://pubs.usgs.gov/sir/2013/5029/.

Goodwin, N.R., Armston, J., Stiller, I., Muir, J., 2016. Assessing the repeatability of terrestrial laser scanning for monitoring gully topography: A case study from Aratula, Queensland, Australia. Geomorphology 262, 24–36. https://doi.org/10.1016/j.geomorph.2016.03.007.

Grams, P.E., Topping, D.J., Schmidt, J.C., Hazel Jr., J.E., Kaplinski, M., 2013. Linking morphodynamic response with sediment mass balance on the Colorado River in Marble Canyon: issues of scale, geomorphic setting, and sampling design. J. Geophys. Res. Earth 118 (2), 361–381. https://doi.org/10.1002/jgrf.20050.

Grams, P.E., Dean, D.J., Walker, A.E., Kasprak, A., Schmidt, J.C., 2020. The roles of flood magnitude and duration in controlling channel width and complexity on the Green River in Canyonlands, Utah, USA. Geomorphology 371, 107438. https://doi.org/10.1016/j.geomorph.2020.107438.

Grams, P.E., Head, E., Mueller, E.R., 2022. Effects of flow regulation and drought on geomorphology and floodplain habitat along the Colorado River in Canyonlands National Park, Utah. River Research and Applications 38 (7), 1266–1276. https://doi.org/10.1002/rra.4014.

Hardy, T., Panja, P., & Mathias, D. (2005). WinXSPRO. *Gen. Tech. Rep. RMRS-GTR-147. Fort Collins, CO: U.S. Department of Agriculture, Forest Service, Rocky Mountain Research Station. 95 p., 147*. doi:https://doi.org/10.2737/RMRS-GTR-147.

Hauer, F.R., Lorang, M.S., 2004. River regulation, decline of ecological resources, and potential for restoration in a semi-arid lands river in the western USA. Aquatic Sciences 2004 66:4 66 (4), 388–401. https://doi.org/10.1007/S00027-004-0724-7.

Hazel, J., Grams, P. E., Schmidt, J. C., & Kaplinski, M. (2010). Sandbar Response in Marble and Grand Canyons, Arizona, Following the 2008 High-Flow Experiment on the Colorado River. https://pubs.usgs.gov/sir/2010/5015/.

Heathfield, D., Walker, I. J., & Grilliot, M. J. (2016). *Comparison of Terrestrial Laser Scanning (TLS) and Structure from Motion (SfM) photogrammetry from unmanned aerial systems (UAS) for geomorphic change detection in beach-dune systems. 2016*, EP21D-0915.

Hereford, R., 1984. Climate and ephemeral-stream processes: Twentieth-century geomorphology and alluvial stratigraphy of the Little Colorado River, Arizona. Geological Society of America Bulletin - GEOL SOC AMER BULL 95. https://doi.org/10.1130/0016-7606(1984)95<654:CAEPTG>2.0.CO;2.

Hohenthal, J., Alho, P., Hyyppä, J., Hyyppä, H., 2011. Laser scanning applications in fluvial studies. Progress in Physical Geography: Earth and Environment 35 (6), 782–809. https://doi.org/10.1177/0309133311414605.

Ismail, A., Ahmad Safuan, A.R., Sa'ari, R., Wahid Rasib, A., Mustaffar, M., Asnida Abdullah, R., Kassim, A., Mohd Yusof, N., Abd Rahaman, N., Kalatehjari, R., 2022. Application of combined terrestrial laser scanning and unmanned aerial vehicle digital photogrammetry method in high rock slope stability analysis: A case study. Measurement 195, 111161. https://doi.org/10.1016/j.measurement.2022.111161.

James, A., Hodgson, M.E., Ghoshal, S., Latiolais, M.M., 2012. Geomorphic change detection using historic maps and DEM differencing: the temporal dimension of geospatial analysis. Geomorphology 137 (1), 181–198. https://doi.org/10.1016/J.GEOMORPH.2010.10.039.

James, M., Robson., 2012. Straightforward reconstruction of 3D surfaces and topography with a camera: Accuracy and geoscience application. J. Geophys. Res. Earth 117 (F3). https://doi.org/10.1029/2011JF002289.

Kasprak, A., Caster, J., Bangen, S.G., Sankey, J.B., 2017. Geomorphic process from topographic form: Automating the interpretation of repeat survey data in river valleys. Earth Surf. Process. Landf. 42 (12), 1872–1883. https://doi.org/10.1002/esp.4143.

Kasprak, A., Bransky, N.D., Sankey, J.B., Caster, J., Sankey, T.T., 2019. The effects of topographic surveying technique and data resolution on the detection and interpretation of geomorphic change. Geomorphology 333, 1–15. https://doi.org/10.1016/J.GEOMORPH.2019.02.020.

Kennedy, J.R., 2023. Aquifer storage change, 2018–2021, in the big Chino Subbasin, Yavapai County, Arizona. In: *Scientific Investigations Report* (2022–5117). U.S. Geological Survey. https://doi.org/10.3133/sir20225117.

KIawon, E. J. (1998). Paleoflood Hydrology and Historic Flood Analysis in the upper Verde River basin, central Arizona. https://repository.arizona.edu/handle/10150/629922.

Lacroix, Mott, Tapia, Elia, Springer, A., 2017. Environmental flows in the desert rivers of the United States and Mexico: Synthesis of available data and gap analysis. J. Arid Environ. 140, 67–78. https://doi.org/10.1016/j.jaridenv.2017.01.011.

Lague, D., 2020. Chapter 8—Terrestrial laser scanner applied to fluvial geomorphology. In: Tarolli, P., Mudd, S.M. (Eds.), Developments in Earth Surface Processes, vol. 23. Elsevier, pp. 231–254. https://doi.org/10.1016/B978-0-444-64177-9.00008-4.

Lane, S.N., James, T.D., Crowell, M.D., 2000. Application of Digital Photogrammetry to complex Topography for Geomorphological Research. Photogramm. Rec. 16 (95), 793–821. https://doi.org/10.1111/0031-868X.00152.

Leica Geosystems, 2017. Leica BLK360 Imaging Scanner. BLK Product Specifications, p. 1. https://shop.leica-geosystems.com/sites/default/files/2019-04/blk360_spec_sheet_2_0.pdf.

Magirl, C.S., Webb, R.H., Griffiths, P.G., 2005. Changes in the water surface profile of the Colorado River in Grand Canyon, Arizona, between 1923 and 2000. Water Resour. Res. 41 (5) https://doi.org/10.1029/2003WR002519.

Major, J.J., Zheng, S., Mosbrucker, A.R., Spicer, K.R., Christianson, T., Thorne, C.R., 2019. Multidecadal Geomorphic Evolution of a Profoundly Disturbed Gravel Bed River System—A complex, Nonlinear Response and its Impact on Sediment delivery. J. Geophys. Res. Earth 124 (5), 1281–1309. https://doi.org/10.1029/2018JF004843.

Manners, R., Schmidt, J., Wheaton, J.M., 2013. Multiscalar model for the determination of spatially explicit riparian vegetation roughness. J. Geophys. Res. Earth 118 (1), 65–83. https://doi.org/10.1029/2011JF002188.

Marjoribanks, T.I., Lague, D., Hardy, R.J., Boothroyd, R.J., Leroux, J., Mony, C., Puijalon, S., 2019. Flexural Rigidity and Shoot Reconfiguration Determine Wake Length behind Saltmarsh Vegetation Patches. J. Geophys. Res. Earth 124 (8), 2176–2196. https://doi.org/10.1029/2019JF005012.

Marshall, P.L., Davis, G., LeMay, V.M., 2000. Using Line Intersect Sampling for Coarse Woody Debris [Technical]. British Columbia Forest Service. Page 2-5. https://www.webpages.uidaho.edu/for373new/pdfs/for373/lineintersectsampling_tr003.pdf.

Merritt, D.M., 2022. 6.15—Reciprocal relations between riparian vegetation, fluvial landforms and channel processes. In: Shroder, J.F. (Ed.), Treatise on Geomorphology, Second edition. Academic Press, pp. 269–297. https://doi.org/10.1016/B978-0-12-818234-5.00001-8.

Molina, A., Govers, G., Cisneros, F., Vanacker, V., 2009. Vegetation and topographic controls on sediment deposition and storage on gully beds in a degraded mountain area. Earth Surf. Process. Landf. 34 (6), 755–767. https://doi.org/10.1002/esp.1747.

National Wild and Scenic Rivers System. (n.d.). Arizona. Retrieved November 6, 2023, from https://www.rivers.gov/arizona.

Neary, D., Medina, A., Baker Jr., M., 2002. Geomorphic Conditions of the Riparian Zona. Upper Verde River.

Neary, D., Medina, A., Rinne, J., Long, J., Baker, M., 2012. Synthesis of Upper Verde River research and monitoring 1993-2008. https://www.fs.usda.gov/research/treesearch/42462.

Notebaert, B., Verstraeten, G., Govers, G., Poesen, J., 2009. Qualitative and quantitative applications of LiDAR imagery in fluvial geomorphology. Earth Surf. Process. Landf. 34 (2), 217–231. https://doi.org/10.1002/ESP.1705.

Overpeck, J.T., Udall, B., 2020. Climate change and the aridification of North America. Proc. Natl. Acad. Sci. U. S. A. 117 (22), 11856–11858.

Passalacqua, P., Belmont, P., Staley, D.M., Simley, J.D., Arrowsmith, J.R., Bode, C.A., Crosby, C., DeLong, S.B., Glenn, N.F., Kelly, S.A., Lague, D., Sangireddy, H., Schaffrath, K., Tarboton, D.G., Wasklewicz, T., Wheaton, J.M., 2015. Analyzing high resolution topography for advancing the understanding of mass and energy transfer through landscapes: A review. Earth Sci. Rev. 148, 174–193. https://doi.org/10.1016/J.EARSCIREV.2015.05.012.

Pool, D., Blasch, K. W., Callegary, J. B., Leake, S. A., & Graser, L. F. (2011). Regional Groundwater-Flow Model of the Redwall-Muav, Coconino, and Alluvial Basin Aquifer Systems of Northern and Central Arizona Scientific Investigations Report 2010-5180, v. 1.1 Prepared in cooperation with the Arizona Department of Water Resources and Yavapai County.

Pörtner, H.-O., Roberts, D. C., Tignor, M. M. B., Poloczanska, E. S., Mintenbeck, K., Alegría, A., Craig, M., Langsdorf, S., Löschke, S., Möller, V., Okem, A., & Rama, B. (Eds.). (2022). Summary for policymakers. In *Climate Change 2022:* Impacts, Adaptation and Vulnerability. *Contribution of Working Group II to the Sixth Assessment Report of the Intergovernmental Panel on Climate Change*. Cambridge University Press.

Pratomo, D.G., Khomsin, Putranto, B.F.E., 2019. Analysis of the green light penetration from Airborne LiDAR Bathymetry in Shallow Water Area. IOP Conference Series: Earth and Environmental Science 389 (1), 012003. https://doi.org/10.1088/1755-1315/389/1/012003.

R Core Team. (2023). *R: The R Project for Statistical Computing* (4.3.0) [Computer software]. R Foundation for Statistical Computing. https://www.r-project.org/.

Ray, G., Megahan, W.F., 1979. Measuring Cross Sections Using a Sag Tape: A Generalized Procedure. USDA.

Rosgen, D.L., 1994. A classification of natural rivers. CATENA 22 (3), 169–199. https://doi.org/10.1016/0341-8162(94)90001-9.

Salehabadi, H., Tarboton, D.G., Udall, B., Wheeler, K.G., Schmidt, J.C., 2022. An Assessment of potential Severe Droughts in the Colorado River Basin [Article]. J. Am. Water Resour. Assoc. 58 (6), 1053–1075. https://doi.org/10.1111/1752-1688.13061.

Sankey, J.B., Ralston, B.E., Grams, P.E., Schmidt, J.C., Cagney, L.E., 2015. Riparian vegetation, Colorado River, and climate: five decades of spatiotemporal dynamics in the Grand Canyon with river regulation. J. Geophys. Res. Biogeo. 120 (8), 1532–1547. https://doi.org/10.1002/2015JG002991.

Sankey, T., Donager, J., McVay, J., Sankey, J.B., 2017. UAV lidar and hyperspectral fusion for forest monitoring in the southwestern USA. Remote Sens. Environ. 195, 30–43. https://doi.org/10.1016/j.rse.2017.04.007.

Sankey, T.Ts., Tango, L., Tatum, J., Sankey, J.B., 2024. Forest fire, thinning, and flood in wildland-urban interface: UAV and lidar-based estimate of natural disaster impacts. Landsc. Ecol. 39 (3), 58. https://doi.org/10.1007/s10980-024-01811-5.

Schenk, E., Jenness, J., Stevens, L., 2018. Springs Distribution, Flow, and Associated Species in the Verde River Basin, Arizona.

Seager, R., Ting, M., Held, I., Kushnir, Y., Lu, J., Vecchi, G., Huang, H.P., Harnik, N., Leetmaa, A., Lau, N.C., Li, C., Velez, J., Naik, N., 2007. Model projections of an imminent transition to a more arid climate in southwestern North America. Science 316 (5828), 1181–1184.

Solazzo, D., Sankey, J.B., Sankey, T.Ts., Munson, S.M., 2018. Mapping and measuring aeolian sand dunes with photogrammetry and LiDAR from unmanned aerial vehicles (UAV) and multispectral satellite imagery on the Paria Plateau, AZ, USA. Geomorphology 319, 174–185. https://doi.org/10.1016/j.geomorph.2018.07.023.

Stromberg, J.C., Stevens, L.E., 2008. Ecological Implications of Verde River Flows. http://vrpartnership.com/.

Stromberg, J.C., Beauchamp, V.B., Dixon, M.D., Lite, S.J., Paradzick, C., 2007. Importance of low-flow and high-flow characteristics to restoration of riparian vegetation along rivers in arid South-Western United States. Freshw. Biol. 52 (4), 651–679. https://doi.org/10.1111/j.1365-2427.2006.01713.x.

Tamminga, A.D., Eaton, B.C., Hugenholtz, C.H., 2015. UAS-based remote sensing of fluvial change following an extreme flood event. Earth Surf. Process. Landf. 40 (11), 1464–1476. https://doi.org/10.1002/ESP.3728.

U.S. Geological Survey, 1998. Revised Methods for Characterizing Stream Habitat in the National Water-Quality Assessment Program. https://doi.org/10.3133/wri984052.

U.S. Geological Survey, 2024a. National Water Information System Database. Clarkdale, AZ. # 09504000. Accessed April 5, 2024. https://doi.org/10.5066/F7P55KJN.

U.S. Geological Survey, 2024b. National Water Information System Database, Paulden, AZ. # 09503700. Accessed April b5, 2024. https://doi.org/10.5066/F7P55KJN.

U.S. National Park Service. (2021, October). What Are Transects, and Why Are They Important for Monitoring Natural Resources? https://www.nps.gov/articles/000/what-are-transects.htm.

Udall, B., Overpeck, J., 2017. The twenty-first century Colorado River hot drought and implications for the future. Water Resour. Res. 53 (3), 2404–2418. https://doi.org/10.1002/2016WR019638.

Van Deusen, P.C., Gove, J.H., 2011. Sampling coarse woody debris along spoked transects. Forestry 84 (2), 93–98. https://doi.org/10.1093/forestry/cpq041.

Walsh, S.J., Butler, D.R., Malanson, G.P., 1998. An overview of scale, pattern, process relationships in geomorphology: A remote sensing and GIS perspective. Geomorphology 21 (3–4), 183–205. https://doi.org/10.1016/S0169-555X(97)00057-3.

Wenger, S., 1999. A Review of the Scientific Literature on Riparian Buffer Width, Extent and Vegetation. Office of Public Service and Outreach. Institute of Ecology, University of Georgia. https://lgpc.ny.gov/system/files/documents/2021/01/buffer_width_p_1999_wenger.pdf.

Wheaton, J.M., Brasington, J., Darby, S.E., Sear, D.A., 2010. Accounting for uncertainty in DEMs from repeat topographic surveys: improved sediment budgets. Earth Surf. Process. Landf. 35 (2), 136–156. https://doi.org/10.1002/ESP.1886.

Williams, A.J., Buck, B.J., Beyene, M.A., 2012. Biological Soil Crusts in the Mojave Desert, USA: Micromorphology and Pedogenesis. Soil Sci. Soc. Am. J. 76 (5), 1685–1695. https://doi.org/10.2136/sssaj2012.0021.

Williams, A.P., Cook, E.R., Smerdon, J.E., Cook, B.I., Abatzoglou, J.T., Bolles, K., Baek, S.H., Badger, A.M., Livneh, B., 2020. Large contribution from anthropogenic warming to an emerging north American megadrought. Science 368 (6488), 314–318.

Wirt, L., 2005. The Verde River Headwaters, Yavapai County, Arizona. *Geologic Framework of Aquifer Units and Ground-Water Flowpaths*. Verde River Headwaters, North-Central Arizona.

Wirt, L., Hjalmarson, H.W., (U.S.), G. S., 2000. Sources of Springs Supplying Base Flow to the Verde River Headwaters. Yavapai County, Arizona.

Wohl, E., 2005. Disconnected rivers: Human impacts to rivers in the United States. In: Ehlen, J., Haneberg, W.C., Larson, R.A. (Eds.), Humans as Geologic Agents, 16. Geological Society of America. https://doi.org/10.1130/2005.4016(03), p. 0.

You, Y., Cao, J., Zhou, W., 2020. A Survey of Change Detection Methods based on Remote Sensing Images for Multi-Source and Multi-Objective scenarios. Remote Sens. (Basel) 12(15), Article 15. https://doi.org/10.3390/rs12152460.

Yousefi, S., Pourghasemi, H.R., Rahmati, O., Keesstra, S., Emami, S.N., Hooke, J., 2021. Geomorphological change detection of an urban meander loop caused by an extreme flood using remote sensing and bathymetry measurements (a case study of Karoon River, Iran). J. Hydrol. 597, 125712 https://doi.org/10.1016/j.jhydrol.2020.125712.

Zaimes, G., Crimmins, M., Green, D., Nichols, M., 2007. Understanding Arizona's Riparian Areas (AZ 1432).. University of Arizona.

Zeileis, A., Grothendieck, G., 2005. Zoo: S3 Infrastructure for regular and Irregular Time Series. J. Stat. Softw. 14, 1–27. https://doi.org/10.18637/jss.v014.i06.